

Supplementary Material

Ubiquitin-dependent DNA damage bypass is separable from genome replication

Yasukazu Daigaku, Adelina A. Davies & Helle D. Ulrich

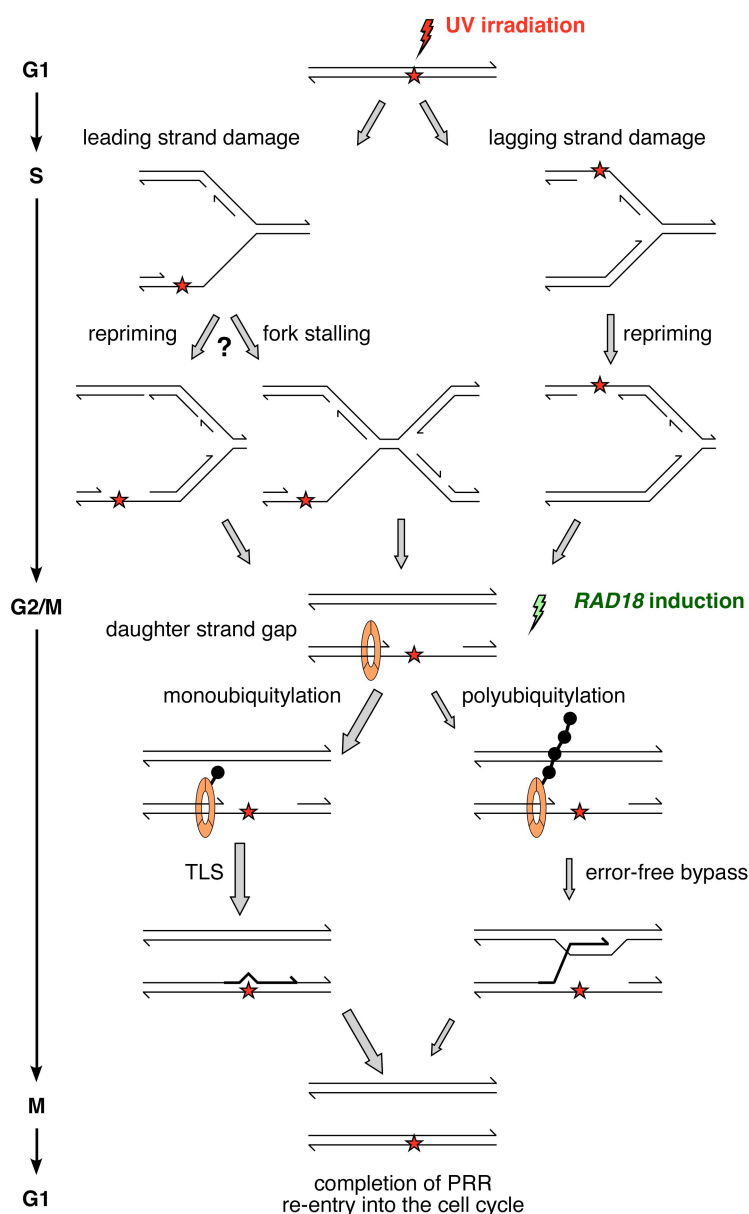


Figure S1. Schematic summary of the experimental setup and the main findings of this study. PRR-deficient cells are UV-irradiated at the G1/S boundary and released into the cell cycle. During the following S phase, unrepaired DNA damage causes replication fork problems. On the leading strand, stalled forks might be reinitiated downstream of a lesion by re-priming, thus leaving a daughter-strand gap. Alternatively, a replication fork from a

neighbouring origin might converge with the stalled fork. On the lagging strand, generation of a new Okazaki fragment downstream of the lesion will also result in a daughter-strand gap. These stretches of unreplicated DNA cause checkpoint activation, thus leading to G2/M arrest. Upon induction of *RAD18* expression, PRR is activated at daughter-strand gaps by means of mono- and polyubiquitylation of PCNA associated with these structures. Damage bypass is achieved predominantly via TLS and to a minor extent by error-free, recombination-dependent template switch. This results in gap filling, deactivation of the checkpoint and re-entry into the cell cycle.

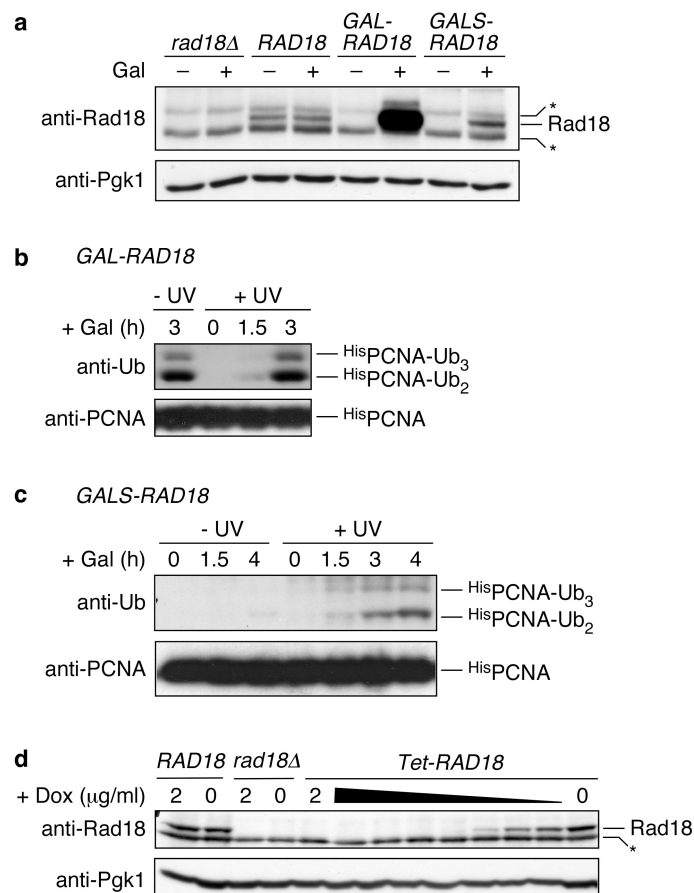


Figure S2. Rad18 protein levels and PCNA ubiquitylation after induction of *RAD18* using regulatable promoters. **a** Western blots of total cell extracts, showing Rad18 protein levels in *RAD18*, *rad18Δ*, *GAL-RAD18* and *GALS-RAD18* cells. Pgk1 was detected as a loading control. **b** Western blots of ^{His}PCNA and its ubiquitylated forms isolated from *GAL-RAD18* cells under denaturing conditions, showing damage-independent ubiquitylation upon induction of *RAD18* expression. **c** Western blots of ^{His}PCNA and its ubiquitylated forms isolated from *GALS-RAD18* cells as above, showing damage-dependent ubiquitylation upon induction of *RAD18* expression. Cells were irradiated with a UV dose of 10 J/m². **d** Western blots of total cell extracts, showing Rad18 protein levels in *RAD18*, *rad18Δ* and *Tet-RAD18* cells grown in the absence or presence of doxycycline at the indicated concentrations. Pgk1 served as a loading control. Asterisks indicate cross-reactive bands detected by the anti-Rad18 antibody.

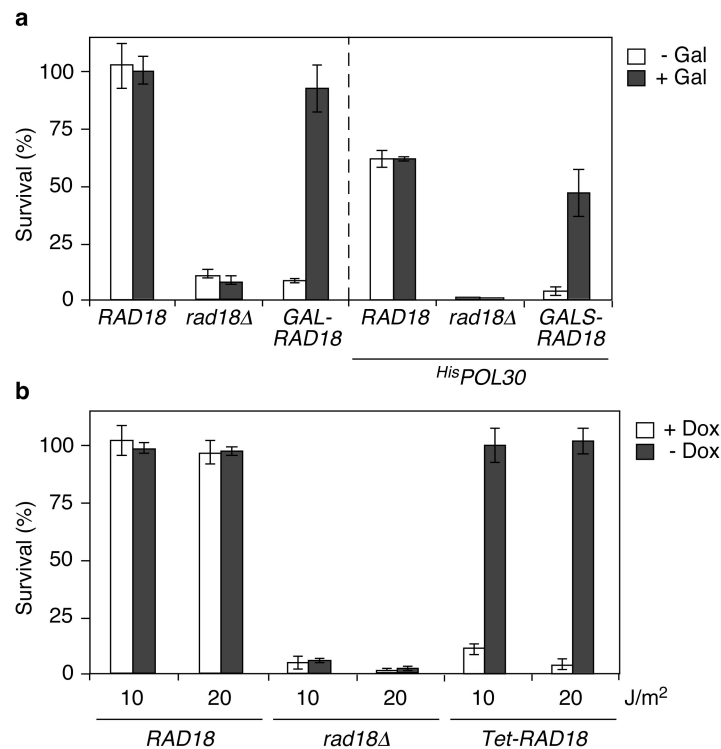


Figure S3. Complementation of UV sensitivities by the inducible *RAD18* constructs used in this study. **a** Characterisation of the galactose-inducible constructs. Survival of the indicated strains was determined after irradiation with 10 J/m² UV (254 nm). Asynchronous logarithmic cultures were grown in the absence or presence of galactose for 2 h before plating onto glucose medium and irradiation. Values are given relative to unirradiated *RAD18* control cultures. Error bars represent standard deviations from up to 6 experiments. Note that the *GALS-RAD18* strain was examined in the *His⁺POL30* background, which causes an overall reduced survival rate. **b** Characterisation of the *Tet-RAD18* construct. The indicated strains were grown overnight in medium containing 2 μg/ml doxycycline, washed and incubated for 3 h in the presence or absence of doxycycline before plating on doxycycline-containing medium and irradiation with 10 or 20 J/m².

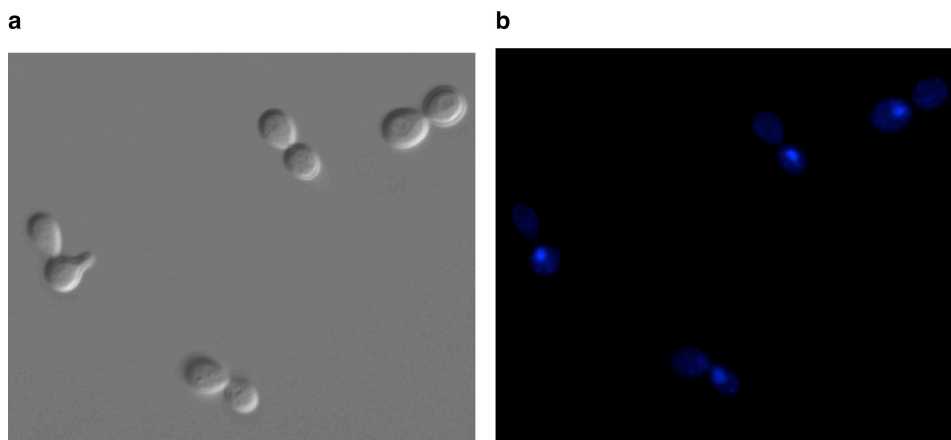


Figure S4. PRR-deficient strains arrest as large-budded G2/M cells upon irradiation at the G1/S boundary. Microscopic images of *GAL-RAD18* cells treated as described in Fig. 1a and grown in the absence of galactose. **a** DIC image of total cells; **b** DAPI-staining of nuclei.

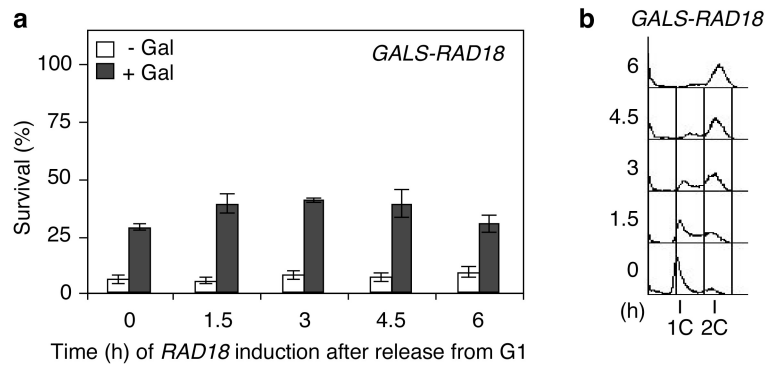


Figure S5. Viability of *GALS-RAD18* cells is not significantly affected by the timing of PRR. Synchronised cells were irradiated in G1/S, and *RAD18* was induced at the indicated time points during and after passage through S phase. **a** Survival rates of *GALS-RAD18* after treatment as described in Fig. 1c. Error bars represent standard deviations from 3 experiments. **b** Cell cycle profile of *GALS-RAD18* cells treated as described in Fig. 1c.

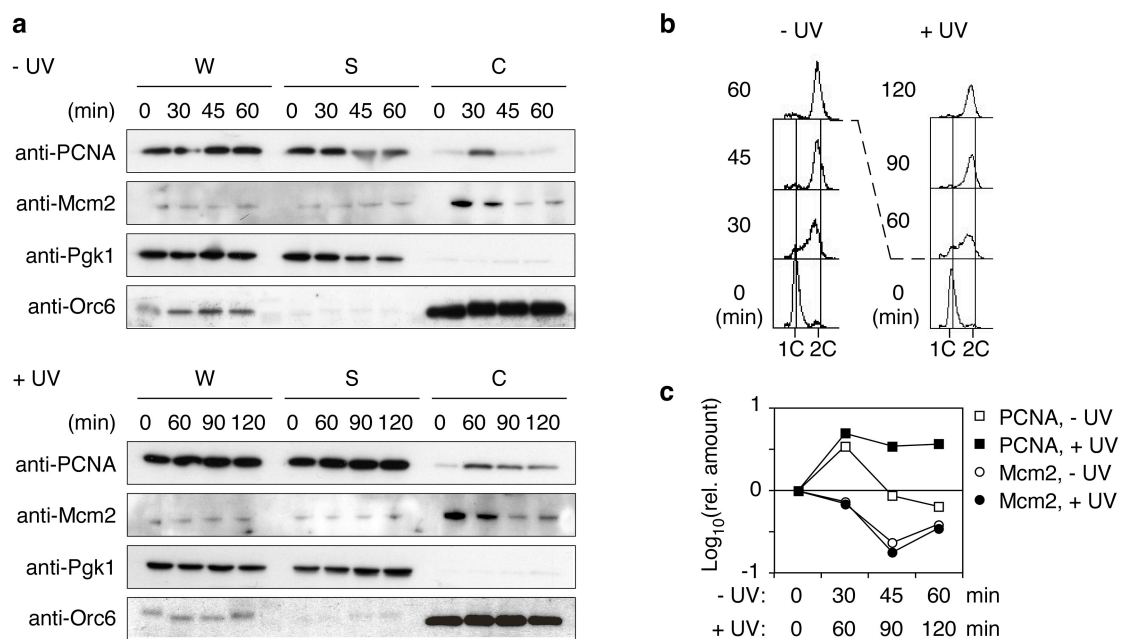


Figure S6. Defects in PRR do not affect cell cycle progression or chromatin association of replication factors. Chromatin-binding assays were performed exactly as in Fig. 2b-d, but using a *rad18Δ* strain and a UV dose of 10 J/m^2 , with comparable results. This indicates that PRR has no significant effect on DNA damage-dependent changes in cell cycle progression or chromatin association of replication factors. **a** Chromatin binding assays. **b** Cell cycle profile of undamaged and irradiated *rad18Δ* cultures. **c** Quantification of the chromatin-associated PCNA and Mcm2 signals from panel b.

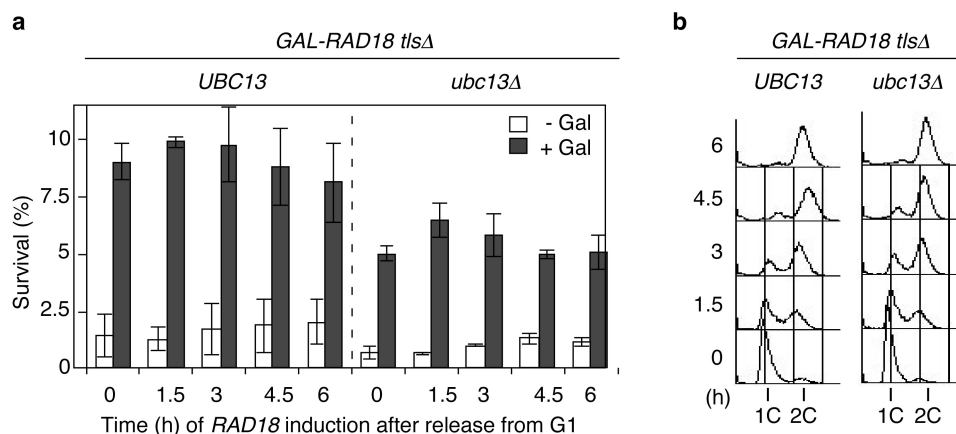


Figure S7. Effect of *ubc13Δ* on viability in a *tlsΔ* background in *GAL-RAD18* cells. Survival assays were carried out with the indicated *GAL-RAD18* strains as described in Fig. 1c. **a** Survival of the indicated strains after induction of *RAD18* during or after S phase, relative to unirradiated controls. Values represent averages and standard deviations from 3 experiments. **b** Cell cycle profile of the indicated strains.

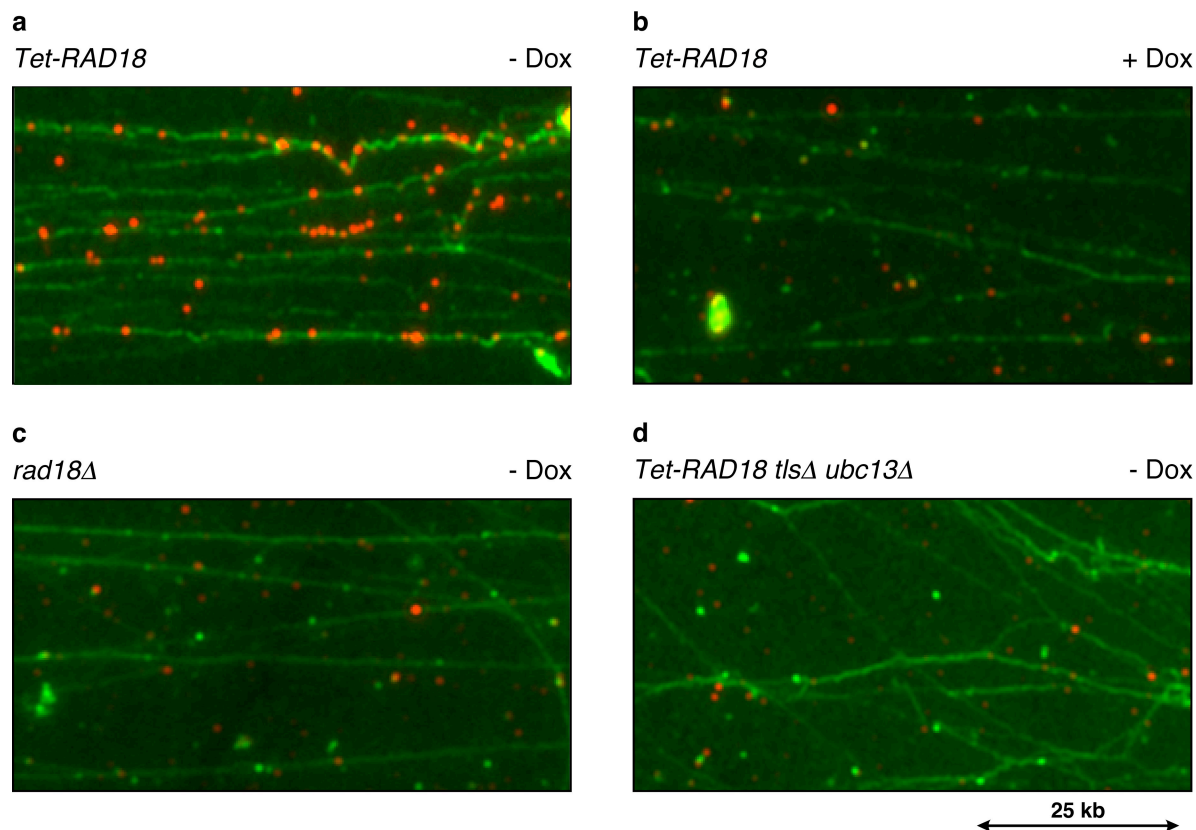


Figure S8. Control images of DNA fibres labeled postreplicatively in the indicated strains. **a** *Tet-RAD18* cells in the absence of doxycycline, i.e. after induction of *RAD18*. **b** *Tet-RAD18* cells in the presence of doxycycline, i.e. under conditions of *RAD18* repression. **c** *rad18Δ* cells, deficient in PRR, in the absence of doxycycline. **d** *Tet-RAD18 tlsΔ ubc13Δ* cells, deficient in PRR, in the absence of doxycycline.

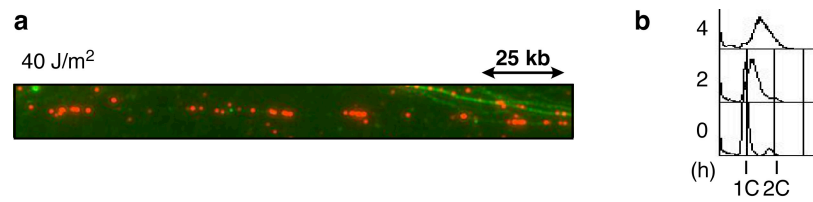


Figure S9. High UV doses prevent completion of S phase in uninduced *Tet-RAD18* cells.
a Fluorescence microscopy image of a DNA fibre labelled postreplicatively in *Tet-RAD18* cells irradiated with 40 J/m². **b** Cell cycle profile of *Tet-RAD18* cells irradiated with 40 J/m² at the G1/S boundary and allowed to enter the cell cycle without *RAD18* induction.

Supplementary References

1. Finley, D., Ozkaynak, E. & Varshavsky, A. The yeast polyubiquitin gene is essential for resistance to high temperatures, starvation, and other stresses. *Cell* **48**, 1035-1046 (1987).
2. Stelter, P. & Ulrich, H. D. Control of spontaneous and damage-induced mutagenesis by SUMO and ubiquitin conjugation. *Nature* **425**, 188-191 (2003).
3. Papouli, E. *et al.* Crosstalk between SUMO and ubiquitin on PCNA is mediated by recruitment of the helicase Srs2p. *Mol. Cell* **19**, 123-133 (2005).

Table S1. Yeast strains used in this study

Strain	Genotype	Reference
<i>WT</i> (DF5)	<i>Mata his3-Δ200 leu2-3,2-112 lys2-801 trp1-1 ura3-52</i>	1
<i>rad18Δ</i>	DF5 <i>rad18::TRP1</i>	2
<i>GAL-RAD18</i>	DF5 <i>rad18::TRP1 URA3::Ylp211-GAL-RAD18</i>	this study
<i>GAL-RAD18 pol30(K164R)</i>	DF5 <i>rad18::TRP1 pol30(K164R) URA3::Ylp211-GAL-RAD18</i>	this study
<i>GAL-RAD18 rad52Δ</i>	DF5 <i>rad18::TRP1 rad52::His3MX URA3::Ylp211-GAL-RAD18</i>	this study
<i>GAL-RAD18 rad14Δ</i>	DF5 <i>rad18::TRP1 rad14::His3MX URA3::Ylp211-GAL-RAD18</i>	this study
<i>GAL-RAD18 tlsΔ</i>	DF5 <i>rad18::TRP1 rev1::URA3 rev3::KanMX rad30::HIS3 URA3::Ylp211-GAL-RAD18</i>	this study
<i>GAL-RAD18 ubc13Δ</i>	DF5 <i>rad18::TRP1 ubc13::HIS3 URA3::Ylp211-GAL-RAD18</i>	this study
<i>GAL-RAD18 tlsΔ ubc13Δ</i>	DF5 <i>rad18::TRP1 rev1::URA3 rev3::KanMX rad30::HIS3 ubc13::HIS3 URA3::Ylp211-GAL-RAD18</i>	this study
^{His} <i>POL30</i>	DF5 <i>pol30::URA3-hisG LEU2::Ylp128-^{His}POL30</i>	2,3
^{His} <i>POL30 rad18Δ</i>	DF5 <i>rad18::TRP1 pol30::URA3-hisG LEU2::Ylp128-^{His}POL30</i>	2,3
^{His} <i>POL30 GAL-RAD18</i>	DF5 <i>rad18::TRP1 pol30::hisG LEU2::Ylp128-^{His}POL30 URA3::Ylp211-GAL-RAD18</i>	this study
^{His} <i>POL30 GALS-RAD18</i>	DF5 <i>pol30::URA3 LEU2::Ylp128-^{His}POL30 rad18::TRP1 KanMX::GALS-RAD18</i>	this study
<i>Tet-RAD18</i>	DF5 <i>KanMX::TetO₇-RAD18 LEU2::TetR'-SSN6</i>	this study
<i>Tet-RAD18 tlsΔ</i>	DF5 <i>rev1::URA3 rev3::KanMX rad30::HIS3 KanMX::TetO₇-RAD18 LEU2::TetR'-SSN6</i>	this study
<i>Tet-RAD18 ubc13Δ</i>	DF5 <i>ubc13::HIS3 KanMX::TetO₇-RAD18 LEU2::TetR'-SSN6</i>	this study
<i>Tet-RAD18 tlsΔ ubc13Δ</i>	DF5 <i>rev1::URA3 rev3::KanMX rad30::HIS3 ubc13::HIS3 KanMX::TetO₇-RAD18 LEU2::TetR'-SSN6</i>	this study
<i>Tet-RAD18 rev1Δ</i>	DF5 <i>rev1::URA3 KanMX::TetO₇-RAD18 LEU2::TetR'-SSN6</i>	this study
<i>Tet-RAD18 rev3Δ</i>	DF5 <i>rev3::KanMX KanMX::TetO₇-RAD18 LEU2::TetR'-SSN6</i>	this study
<i>Tet-RAD18 rad30Δ</i>	DF5 <i>rad30::HIS3 KanMX::TetO₇-RAD18 LEU2::TetR'-SSN6</i>	this study
<i>BrdU*</i>	DF5 <i>URA3::p306-BrdU-Inc</i>	this study
<i>BrdU* rad18Δ</i>	<i>BrdU* rad18::TRP1</i>	this study
<i>BrdU* Tet-RAD18</i>	<i>BrdU* KanMX::TetO₇-RAD18 LEU2::TetR'-SSN6</i>	this study
<i>BrdU* Tet-RAD18 tlsΔ</i>	<i>BrdU* rev1::URA3 rev3::KanMX rad30::HIS3 KanMX::TetO₇-RAD18 LEU2::TetR'-SSN6</i>	this study
<i>BrdU* Tet-RAD18 ubc13Δ</i>	<i>BrdU* ubc13::HIS3 KanMX::TetO₇-RAD18 LEU2::TetR'-SSN6</i>	this study
<i>BrdU* Tet-RAD18 tlsΔ ubc13Δ</i>	<i>BrdU* rev1::URA3 rev3::KanMX rad30::HIS3 KanMX::TetO₇-RAD18 LEU2::TetR'-SSN6</i>	this study
<i>BrdU* Tet-RAD18 rev1Δ</i>	<i>BrdU* rev1::URA3 KanMX::TetO₇-RAD18 LEU2::TetR'-SSN6</i>	this study
<i>BrdU* Tet-RAD18 rev3Δ</i>	<i>BrdU* rev3::KanMX KanMX::TetO₇-RAD18 LEU2::TetR'-SSN6</i>	this study
<i>BrdU* Tet-RAD18 rad30Δ</i>	<i>BrdU* rad30::HIS3 KanMX::TetO₇-RAD18 LEU2::TetR'-SSN6</i>	this study